

## Vacuum Ultraviolet Absorption Measurements of Ground State Xenon in the Near Field of a Low Power Hall Thruster

M. A. Cappelli<sup>†</sup>

Mechanical Engineering Department, Stanford University, Stanford, California

W. A. Hargus, Jr.<sup>‡</sup>

Air Force Research Laboratory, Edwards Air Force Base, California

### Abstract

Measurements are presented for the density of ground-state neutral xenon atoms in the near field of a 200W co-axial Hall thruster. The diagnostic strategy employed is a variation of a classical absorption technique, using retro-reflected intrinsic line emission from the resonance 147 nm vacuum ultraviolet (VUV) transition in atomic xenon as a source for absorption. In this way the technique has, in principal, the sensitivity of narrow-band absorption methods. Preliminary values for the near field number density ( $10^{19} - 10^{20} \text{m}^{-3}$ ) are within range of those expected. The limitation in sensitivity and accuracy is due largely to a weak reflected emission beam, resulting primarily from losses in the optical components. Future experiments will make use of fully reflective optics, which provides easier alignment in the visible, and improved optical throughput in the 147 nm region studied.

### I. Introduction

Little is presently known of the near-field properties of Hall thrusters. While plasma properties such as electrostatic potential, temperature, and ion velocities can be measured using either electrostatic probes or laser probing of excited electronic states of xenon, the density of the neutral xenon ground electronic state is rather elusive. This is largely due to the low densities ( $\sim 10^{19} \text{m}^{-3}$ ) and inaccessibility by optical probing as a result of the large excitation energy (8.5 eV). Knowledge of the xenon density in the near field is critical to the development of thruster simulations, in particular, if one is attempting to capture the current-voltage behavior of the thruster discharge. At low voltages, where the propellant is not yet fully ionized, increases in voltage lead to dramatic increases in total discharge current, most likely due to the increased rate and level of ionization. At high voltages, the current nearly saturates, as the propellant has become completely ionized. An increase in current in this current saturation regime would require a change in the effective resistivity of the discharge. This resistivity change could come about through interactions of the plasma electrons with the channel wall, fluctuations in the electric and magnetic field (plasma

turbulence), or scattering collisions with the background neutral ground-state xenon (classical resistivity). Characterizing the latter requires an estimate of the near-field neutral xenon number density, which has not yet been directly measured in any Hall discharge.

This report serves to describe preliminary measurements of xenon density obtained in the near field of a 200W Busek Hall thruster, operating in Chamber 6, at the Air Force Research Laboratory (AFRL) Electric Propulsion Research Facility at Edwards Air Force Base, in California. The approach taken is to measure the radiative transfer characteristics of the intrinsic resonance transition ( $5p^6 (^1S_0) - 5p^5 6s (^3P_1)$ ) centered at 146.97 nm. This measurement required the application of vacuum ultraviolet spectroscopy. Details of the theory and experimental approach are provided below.

### II. Background

The most straightforward method of measuring xenon ground state atomic species number density,  $n_{Xe}$ , is either by broadband or narrowband vacuum ultraviolet spectroscopy. With this method, radiation (generated either by a mini-arc lamp for broadband diagnostics, or a low pressure glow discharge for narrowband diagnostics) in the vicinity of the  $5p^6 (^1S_0) - 6s (^3P_1)$  transition in neutral xenon (XeI) about a wavelength of 146.97 nm is passed through the plasma plume of the Hall thruster, in the near field of the exit plane. The transmitted radiation is imaged onto the entrance slit of a vacuum monochromator for spectral discrimination, or straight onto a VUV

---

<sup>†</sup> Associate Professor, Member AIAA

<sup>‡</sup> Senior Member AIAA

Copyright © by Stanford University. Published by the American Institute of Aeronautics and Astronautics, Inc. with permission.

photodetector for narrowband absorption. The intensity of the transmitted beam relative to that incident onto the plasma is a direct measure of the number of absorbers present. Knowledge of the detailed optical constants (e.g., line strength and broadening rates) makes this an absolute measurement not necessarily requiring calibration for physical constants. In principal, there is no limit to the sensitivity that can be achieved in this measurement, although experimental drifts and finite integration times (to overcome photon statistics) limits these types of absorption measurements on atomic resonance lines to densities above about  $10^{18}$ - $10^{20}$   $\text{m}^{-3}$ . These densities are in the range of those expected in a Hall thruster exit region, based on indirect measurements carried out at Stanford University with much more sophisticated diagnostic methods.

In our first examination of vacuum ultraviolet spectroscopy, it was determined that absorption measurements using a broadband arc lamp source were not sufficiently sensitive to the range of density expected, as a result of (i) drifts/fluctuations in the arc lamp intensity detected in the range of 1-10 Hz, and (ii) limited resolution of the monochromator, which was used to resolve the absorption hole generated by the ground state xenon absorbers. An alternate strategy was therefore implemented, which has proven to be moderately effective. As shown below, preliminary measurements and analysis give extracted exit field number densities that are in the expected range for Hall thrusters.

The absorption strategy that was employed is referred to here as a reflection – reabsorption method. This method is a variation of a narrow band absorption technique performed using the intrinsic emission from the plasma that is being probed, as the spectrally-narrow probe beam itself. An illustrative schematic of this method is given in Figure 1. For the sake of describing this approach, we shall use a uniform plasma source as an example of the plasma being interrogated. Basically, a measurement is made of the (spectrally unresolved) emission associated with the resonance transition as shown in Figure 1a). The signal associated with this is referred to as the direct emission,  $S_{DE}$ . This emission may be optically thick for the line of interest, and so for a uniform plasma source, will have a distorted spectral shape that asymptotically approaches the Planck distribution beginning near its spectral line center. A second measurement is made of the resonance

emission that propagates in the opposite direction to that in Figure 1a), but reflected so that it retraces its path through the plasma into the optical path originally used for emission (see Figure 1b). The spectral signature of this emission source will be characterized by reduced intensity near the transition line center, owing to absorption by the neutral xenon. The signal associated with this is referred to as the reflected emission,  $S_{RE}$ . In practice, both measurements are made simultaneously, using optics shared by both paths. The measurements are coincident, and are distinguished from each other by using phase sensitive detection.

In Figure 1a) a chopper is used to modulate the direct emission at a frequency  $\omega_{DE}$ . In Figure 1b), a second chopper is used to modulate the reflected emission at a frequency  $\omega_{RE}$ . Two lock-in amplifiers serve to separate the signals on a single detector. As discussed below, the ratio of the signal  $R = S_{RE} / S_{DE}$  is a function of the ground state neutral xenon number density. It is apparent that if the geometric collection efficiencies of the two optical trains are equal (including the assumption of ideal reflection from the mirror in Figure 1b)), and if the plasma is optically thin (i.e., sufficiently low density such that absorption of the spectral line radiation is negligible), then the ratio  $R$  must approach unity. In fact, the signal obtained from a *non-resonance spectral line*, as the optical train passes through the edge of the plasma, serves as a means of calibrating differences in the collection efficiencies of the two optical trains.

The major drawback of this method is that measurements can only be made of a luminous plasma (since its emission serves as the probe itself). This did not prove to be an impediment here, in the measurements where confined to the annular plasma region of the near field of a coaxial Hall thruster.

In the background theory described below, it is assumed that the background xenon in the chamber does not contribute to the absorption of the resonance line in either of the two branches. The effect of the background pressure will serve to reduce the signals  $S_{RE}$  and  $S_{DE}$ . In the actual analysis of the data, the background density is taken into account. The background number density is sensitive to the ratio  $S_{RE} / S_{DE}$  detected at large distances off axis. In the absence of background xenon, this ratio should approach unity, as both paths should lead to optically thin radiative transport.

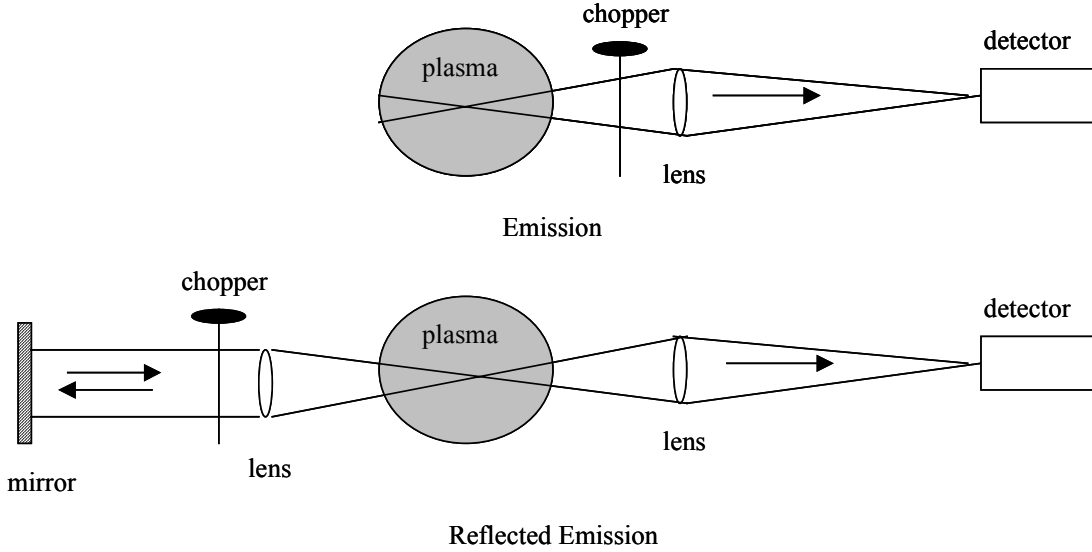


**Figure 1:** (a) top-conventional emission measurement. (b) bottom-absorption of the reflected emission, redirected through the plasma opposite the direction of the direct emission.

### III. Theory

The spectral irradiance emitted by a hot plasma of uniform excitation temperature<sup>†</sup> but non-uniform absorption coefficient along a direction  $z$ , over a path length  $L$  is [1]:

$$I_{\omega_{DE}} = I_{\omega_p} \left( 1 - \exp \left( - \int_0^L \kappa_{\omega} dz \right) \right) \quad [1]$$

Here,  $I_{\omega_p}$  is the Planck function, which describes the isotropic thermal radiation field at the excitation temperature of the resonance state, and  $\kappa_{\omega}$  is the spectral absorption coefficient for the resonance transition ( $1 \rightarrow 2$ ), which is given as:

$$\kappa_{\omega} = \frac{h\omega}{8\pi^2} B_{12} N_1 \phi_{12}(\omega) \quad [2]$$

$N_1$  ( $\approx n_{Xe}$ ) is the ground state xenon number density,  $\phi_{12}$  is the transition lineshape, and  $B_{12}$  is the Einstein stimulated absorption coefficient, given as:

<sup>†</sup> The assumption of a uniform excitation temperature greatly simplifies the analysis, and, based on probe measurements at the exit of Hall discharges, is expected to lead to only a small error in the measured density, in comparison to other experimental uncertainties.

$$B_{12} = \frac{4\pi^3 e^2 f_{12}}{\epsilon_0 h m_e \omega_{12} c} \quad [3]$$

where  $f_{12} = 0.264$  [2] is the transition absorption oscillator strength, and all other symbols represent the usual atomic constants.

The resonance transition lineshape is assumed to be Doppler, resonance, and lifetime-broadened. It is noteworthy that the resonance transition in xenon is subject to hyperfine splitting due to electron angular momentum coupling to the nucleus, as well as isotopic shifting due to variations in the term energies for different isotope masses. For spectral features that are much broader than the hyperfine structure, the hyperfine structure can be considered as an additional broadening component. The optical constants associated with these shifts are largely unknown for this transition, though a recent study by Anderson et al [2] assigns the broadening associated with this transition to  $< 0.9 \text{ cm}^{-1}$ . Our analysis and results presented in this paper find that the estimated xenon densities are moderately sensitive to the estimated hyperfine structure, and a value of  $0.9 \text{ cm}^{-1}$  was used for the data presented. Future analysis will examine the effects, if any, of hyperfine splitting, using optical constants from similar, analogous transitions in xenon.

If the spectral irradiance given by Eqn. [1] is redirected back through the plasma, then this irradiance serves as a background source, which will be further attenuated in accordance with Beer's Law:

$$I_{\omega_{RE}} = I_{\omega_p} \left( 1 - \exp \left( - \int_0^L \kappa_{\omega} dz \right) \right) \exp \left( - \int_0^L \kappa_{\omega} dz \right) \quad [4]$$

At this point, some simplifications are noteworthy, and, for the purpose of a preliminary analysis, are warranted. We shall assume that the plasma is uniform along the length  $L$ , and that over the spectral range of the transition, the Planck function does not vary substantially. Both of these conditions can be relaxed, for a more detailed analysis but serve to illustrate the usefulness of this diagnostic here. Also, we shall integrate over a spectral bandwidth,  $\Delta\omega$ , as it is assumed that the monochromator involved in isolating the resonance transition serves primarily as a spectral filter (i.e., does not scan over the emission/absorption feature to resolve the structure). Under these circumstances, Eqns. [1] and [4], when spectrally integrated, reduce to:

$$I_{DE} = I_{\omega_p}(\omega_{12}) \int_{\omega_{12}-\Delta\omega/2}^{\omega_{12}+\Delta\omega/2} (1 - \exp(-\kappa_{\omega}(\omega)L)) d\omega \quad [5]$$

$$I_{RE} = I_{\omega_p}(\omega_{12}) \int_{\omega_{12}-\Delta\omega/2}^{\omega_{12}+\Delta\omega/2} (1 - \exp(-\kappa_{\omega}(\omega)L)) \times \exp(-\kappa_{\omega}(\omega)L) d\omega \quad [6]$$

The actual signals detected will be proportional to some geometric, spectral, and electronic conversion factors,  $G_{DE}$  and  $G_{RE}$ , which can be different for the two branches:

$$S_{DE} = G_{DE} I_{DE} \quad [7a]$$

$$S_{RE} = G_{RE} I_{RE} \quad [7b]$$

The signal ratio:

$$R = \frac{S_{DE}}{S_{RE}} = C_R \frac{I_{DE}}{I_{RE}} \quad [8]$$

with  $C_R = G_{DE}/G_{RE}$  a constant that can be determined, as discussed above, by evaluating the ratio as it passes through a chord of the co-axially symmetric Hall discharge plasma that is either very short ( $L \rightarrow 0$ ), or is optically thin to the emitted and

reflected spectral line ( $\kappa_{\omega}L \ll 1$ ). However, this ratio is expected to be unity only in the absence of absorption due to background xenon in the chamber. Since there is a finite amount of background xenon in the chamber (some  $10^{-6}$  Torr during operation), a was performed using spectral emission lines (e.g., from boron (BI) or for ionized xenon (XeII)) that are expected to be optically thin.

For purposes of illustration, we plot in Figure 2, the normalized spectral irradiance (integrands of Eqns. [5] and [6]),  $I_{\omega_{DE}}/I_{\omega_p}(\omega_{12})$  in 2a) and  $I_{\omega_{RE}}/I_{\omega_p}(\omega_{12})$  in 2b) that is expected to be directly emitted and re-transmitted through the plume. In this example calculation, we have assumed a xenon gas temperature of 1000K, a plasma path length of  $L = 0.06$  m, and a xenon ground state number density of  $N = 10^{20} \text{ m}^{-3}$ . It is apparent that while the direct emission saturates near the spectral line center to the Planck radiation limit, the reflected emission that is re-transmitted through the plasma suffers re-absorption and the depletion of its spectral line core. The ratio of the integrated emission for these two cases (assuming  $C_R = 1$ ), as the ground state xenon density is varied, is given in Figure 3. We see that the ratio varies modestly with xenon gas density, and depends on the path length (as expected), rendering this measurement suitable as a diagnostic over the expected xenon density range. Because the broadening is dominated by the hyperfine splitting, the ratio is not found to be very sensitive to the gas temperature.

In the analysis of the experimental data presented below, we first assume that the plasma is uniform within a disk across the discharge exit plane of

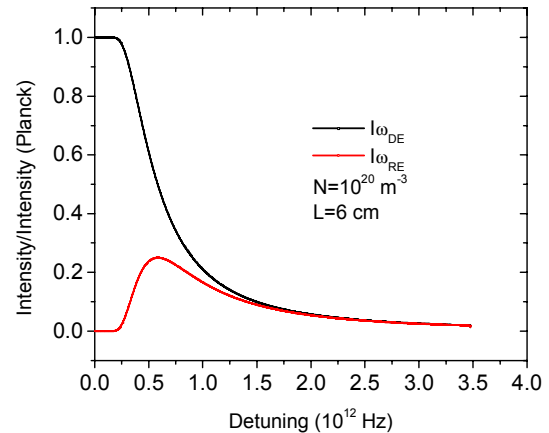


**Figure 2:** Spectral shape of the directly emitted spectral line ( $I_{\omega_{DE}}$ ), and of the reflected ( $I_{\omega_{RE}}$ ) resonance line that is re-directed through the uniform 6 cm - long path of plasma.

radius,  $r_o$ . This disk radius is adjusted in a radiation transport calculation to generate a lateral variation in the ratio,  $R$ , that best fits with the measured lateral distribution in the experiment. For regions very close to the exit plane, this model may not be appropriate, as the neutral density should occupy a ring coincident with the channel dimensions that correspond to the location of the inner and outer channel walls, respectively. However, because of the geometry of the Hall thruster studied here, the presence of an extended inner pole piece precluded measurements across the entire exit plane very close to the thruster exit. The analysis of the data however, did require the solution of the radiative transfer equation for an assumed annular geometry, accounting for the absorption due to the background xenon in the chamber, and adjusting the assumed disk size and uniform disk density until favorable agreement was seen between the predicted and observed lateral scans in the ration  $R$ .

## II. Experiment

A detailed schematic of the measurements that were carried out and described here is illustrated in Figure 4. In the schematic, the Hall thruster is co-axial and shown firing towards the reader, centered in the vacuum chamber. The Hall thruster studied here belongs to the family of Busek BHT-200 thrusters, which nominally run at a power of approximately 200W. It has an inner wall diameter of 15 mm, and an outer wall diameter of 31 mm (8 mm channel width). The central pole piece extended approximately 7 mm beyond the exit plane of the channel. The tip of the pole piece served as the origin position marker for the axial position referred to in the measurements. The cathode was located approximately 20 mm downstream of the central pole

piece. Measurements were performed in Chamber 6 at the Air Force Research Laboratory Electric Propulsion Facility (Edwards AFB). The chamber is 1.8 m in diameter and 3 m long with a measured pumping speed of  $\sim 32,000$  l/s on xenon, provided by four single-stage cryo panels and one 50 cm diameter two-stage cryo-pump.

A 2.54 cm diameter  $MgF_2$  lens inside the tank having an effective focal length of 26.87 cm (and positioned 26.87 cm from the thruster geometric center) served to collect and collimate the direct emission, which is chopped for phase-sensitive detection at a frequency  $\omega_{DE}$ . A second lens of the same characteristics collects the same emission along a direction opposite to that of the direct emission, collimates it and redirects it back to retrace its path through the plasma using an ultraviolet sensitive mirror. This emission then falls on the first lens, and is re-collimated to be coincident with the path of the direct emission. In order to distinguish this resonance emission from the direct emission, it is chopped at a different frequency,  $\omega_{RE}$ . Both the direct emission and the reflected emission, which are collimated while inside the chamber, are focused onto the entrance slit of a  $\frac{3}{4}$  m vacuum monochromator using a 21 cm focal length, 2.54 cm diameter  $MgF_2$  lens. A continuous vacuum interface is facilitated through the use of flexible vacuum bellows, which support the lens. Other dimensions (e.g., placement of choppers and mirror) are not critical. For the measurements described here, the entrance and exit slits of the monochromator were set to 100  $\mu m$ , providing a spectral resolution of approximately 0.1 nm. A solar blind photomultiplier is used to provide a signal proportional to intensity falling on the exit slit. This signal is sent to the lock-in amplifier for further analysis.

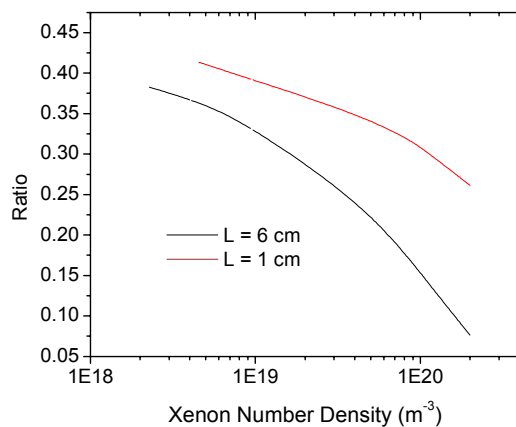


**Figure 3:** Integrated intensity ratio,  $R$ , with  $C_R=1$ , as the background neutral xenon number density is varied. Shown are calculations for 1000K and two cases of neutral xenon path length:  $L = 6$  cm, and  $L = 1$  cm.

## IV. Results

Experiments were carried out after careful alignment of the optical paths for concentricity, with the vacuum chamber open. The thruster has channel dimensions of 31 mm diameter (outer wall), and 15 mm diameter inner wall, and has a conically shaped insulating cone that protrudes a distance of 7 mm from the exit of the channel. The thruster was operated at nominal conditions ( $I = 0.82$  A,  $V = 250$  V, mass flow rate = 8.5 sccm (anode), 1 sccm (cathode)). During operation under these conditions, the background pressure as recorded by an ionization gage (uncorrected for xenon) was found to be about  $5 \times 10^{-6}$  Torr. For the results presented here, the emission path traverses the plume at an axial position  $z$  defined by the distance away from the tip of the conically shaped cone. The thruster is translated laterally (along a direction normal to the thrust axis

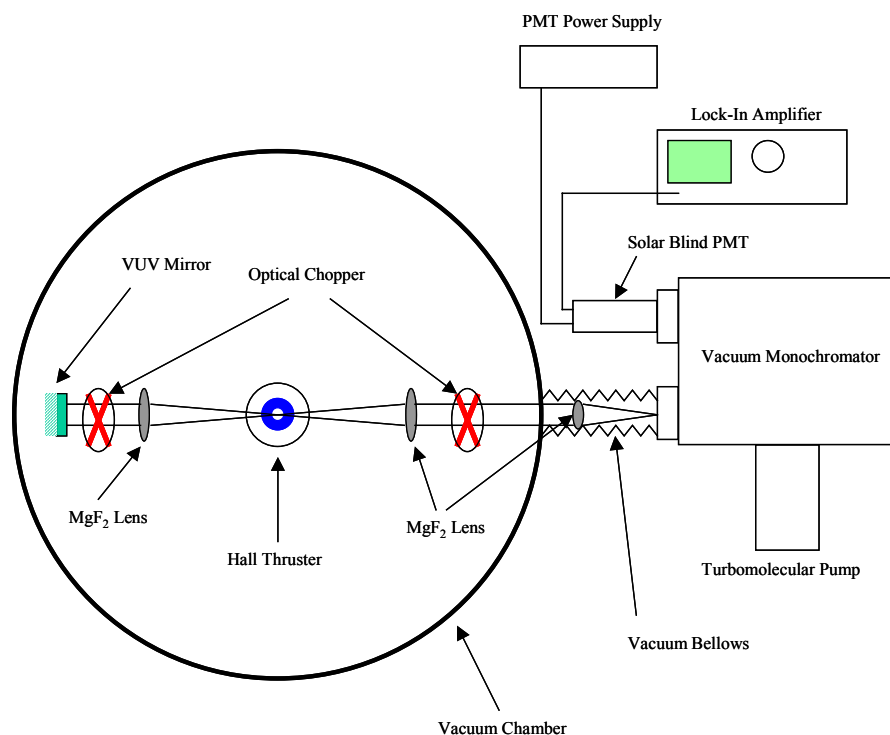


Figure 4: Experimental Schematic.

and emission path) so that the emission traverses laterally across the plume along various chords. For the experiments presented here, the calibration factor,  $C_R = 0.03 (\pm 0.02)$ , was determined from an average of estimates made using either a nearby BI line, centered at approximately 137 nm, and a nearby Xe ion line, centered at approximately 125 nm. The determination of this calibration was probably the single most important measurement limiting the absolute accuracy of this diagnostic.

Representative signals from both the direct emission, and the reflected retransmitted emission are shown in Figure 5, taken with the thruster operating in a “glow discharge” mode, i.e., with the current to the magnets turned off. These are spatial scans taken by lateral (vertical) translation of the Hall thruster. It is apparent that the overall quality of the direct emission is much higher than that of the reflected emission, most likely due to additional losses introduced by the extra optical components. Overall, however, the two shapes are similar.

Figure 6 displays the resulting ratio, corrected for the relative path sensitivity using  $C_R = 0.03$ . Also shown in Figure 6 is a 50-point average, which smoothens the signal due to random fluctuations in the reflected emission path intensity. It is noteworthy that negative values for the lateral position correspond to the side of the plume opposite the placement of the cathode (positive lateral coordinate). It is suspected that for lateral positions greater than

about 25 mm, there may be a distortion in the observed emission on either or both paths, due to the presence of the interfering cathode. For this reason, data beyond approximately 20 mm should be least trusted. It is also noteworthy that the use of  $C_R = 0.03$  gives an intensity ratio that approaches unity ( $R = 1$ ) at a lateral position of approximately -70 mm (57 mm from the axis opposite the cathode placement), as expected, since emission passing through a chord across the periphery of the plasma plume should be optically thin.

The general shape associated with the signal ratio  $R$  versus lateral position is not surprising. Low

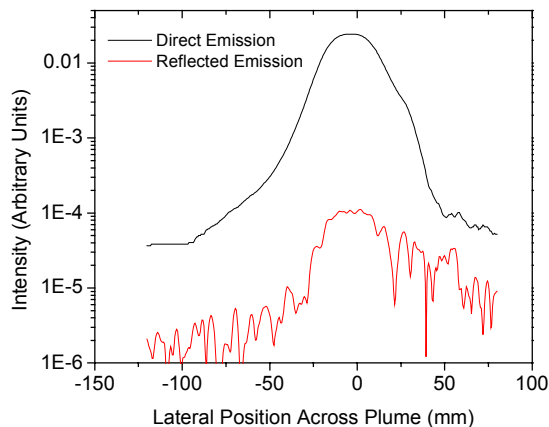
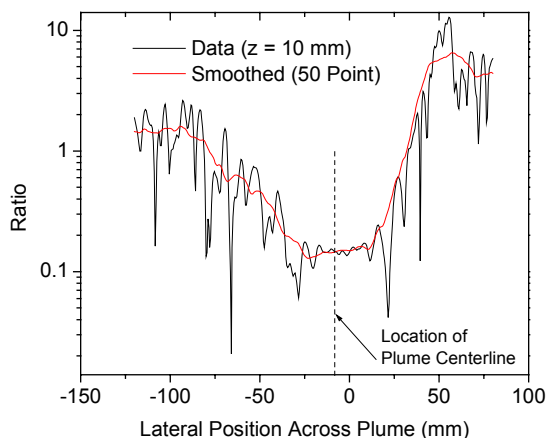


Figure 5. Typical lateral emission scans,  $z = 10$  mm (1 cm downstream of the central pole-piece extension).

values near the axis ( $R \approx 0.1$ ) correspond to ground state xenon number densities of  $> 1 \times 10^{20} \text{ m}^{-3}$  (assuming  $L=6 \text{ cm}$ ), in accordance with the results of the calculations shown in Figure 3 above. The width of this spatial absorption profile suggests that the breadth of the plume (extent over which significant absorption may be taking place) extends beyond 50 mm from the axis, even though the outer channel dimension has a radius of 15.5 mm. It appears that there is considerable neutral xenon expansion (divergence) well beyond the radius of the channel, even at a relatively short axial location of  $z = 10 \text{ mm}$ .

Figure 7 compares the ratio of the signals obtained with the magnets to the discharge on ( $I_M = 1 \text{ A}$ ), and with the magnets off. Turning the magnets on is seen to result in an increased value for the ratio in the core. This is expected, since absorption is expected to diminish as the now energetic plasma



**Figure 6.** Ratio,  $R$ , of the data in Figure 5 determined for a calibration constant of  $C_R = 0.03$ . Also shown is a 50 point smoothing of the data.

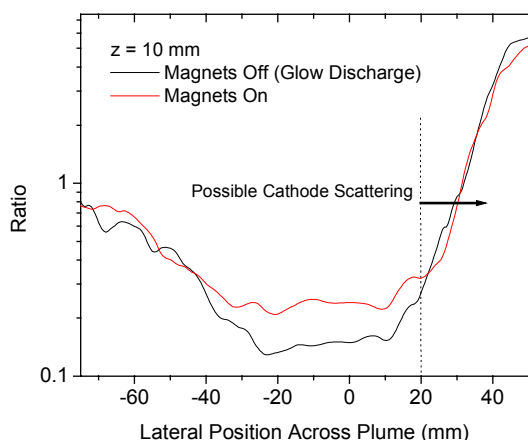


**Figure 7.** Ratio for the same axial positions, with the magnets off (discharge in glow mode), and with the magnets on.

depletes the xenon ground state species. The estimated number density of the ground state xenon is reduced to about  $4 \times 10^{19} \text{ m}^{-3}$ , based on the calculations of Figure 3. While these numbers seem to be on the high side of those expected, on the basis of the known mass flow rate and an estimate of the neutral flow velocity (assumed to be choked channel flow), they agree within the estimated experimental uncertainty, which is about a factor of 2-4, due mainly to the uncertainty in the calibration constant, and to the poor signal-to-noise on the return, retro-reflected path.

The analysis of the raw data involved solving the radiation transfer equation for a uniform disk of ground state xenon absorbers, as the direct emission and reflected, re-transmitted emission pass through varying (lateral) chords across the plume. The analysis also accounts for the low density background xenon which adds approximately one meter of absorption to the direct emission, and two meters to the reflected emission, based on the placement of the optics. Figure 8 presents a typical comparison of the simulated lateral variation in the intensity ratio,  $R$ , to that measured experimentally. The simulated intensity ratio depicts the general behavior seen in the sigmoidal fit to the experimental data. The simulations rise more quickly near the plume edge, mainly due to the assumed step-decrease in the xenon density at the disk edge.

For the typical result seen in Figure 8, the plume properties that best agree with the experiments correspond to a neutral density of  $4 \times 10^{19} \text{ m}^{-3}$ , a background density of  $10^{16} \text{ m}^{-3}$ , and a plume diameter of 11.2 cm. The plume density was determined mainly by the ratio at the base of the profile, the plume diameter by the lateral location in the rise in

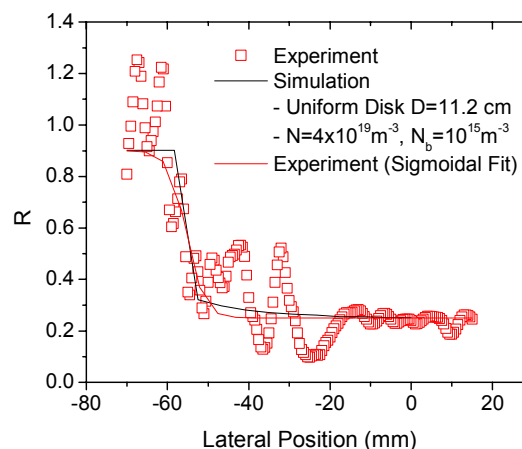


**Figure 8.** Typical signal ratio, comparing the raw data to a sigmoidal fit to the data, and to the results of the simulations, assuming a uniform disk of absorbing xenon.

this ratio, and the background density by the value in the ratio at the plume edge.

Figures 9 and 10 present the overall results, analyzed in accordance with the procedure described above and depicted in Fig. 8. The plume density is seen to fall off rapidly, by nearly a factor of ten, within two centimeters of the exit plane of the thruster, attributable to a rapid expansion of the neutral fluid. As seen in Fig. 9, when the magnets to the thruster are turned off, the xenon number density increases as a result of a reduction in the degree of ionization. The rise in density (by a factor of 2) suggests that the plasma is approximately 50% ionized, though the experimental uncertainty of at least a factor of 2 in number density precludes any significant assessment of the degree of ionization in the Hall thruster plume at this time.

The effective radius of the neutral plume is shown in Fig. 10. As noted above, the axial position is measured relative to the tip of the cap on the central pole piece, which protrudes approximately 7 mm beyond the exit of the discharge channel. It is apparent that within about 2 cm from the exit plane

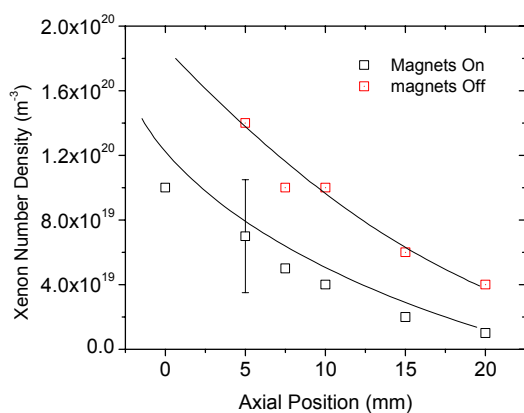


**Figure 9.** Axial variation in the neutral xenon density (assumed uniform across the plume).

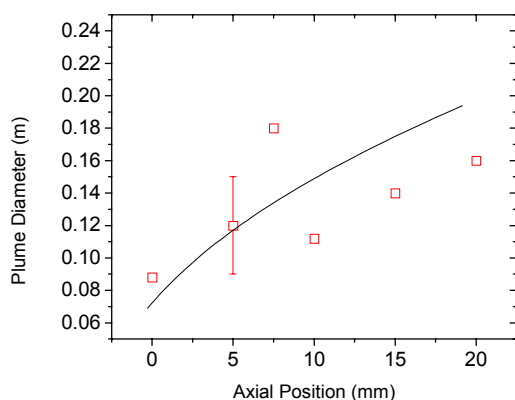


**Figure 10.** Axial variation in the effective neutral xenon plume diameter.

of the thruster, the neutral plume has expanded to a diameter of about 20 cm, or six times the channel diameter, based on the diameter of the outer insulator of the co-axial channel (3.1 cm). A point source expansion would predict the density to drop by a factor of about thirty-six, in reasonable agreement with the trend seen in Figure 9. These results, though preliminary, confirm the general expectation that the neutral flow expands rapidly beyond the exit plane, and, for the first time, provides an estimate of the near field density in the region of the plasma where the electron conductivity is anomalous.

## VI. Summary

This paper presents the first result of a novel VUV absorption technique applied to the measurement of neutral xenon density in the near field of a Hall thruster. The approach taken is to measure the radiative transfer characteristics of the intrinsic resonance transition ( $5p^6 (^1S_0) - 5p^5 6s (^3P_1)$ ) centered at 146.97 nm. The absorption strategy that was employed is referred to as a reflection – reabsorption method. This method is a variation of a narrow band absorption technique performed using the intrinsic emission from the plasma that is being probed, as the spectrally-narrow probe beam itself. This study serves to provide: (i) a first estimate on the viability of this diagnostic, (ii), preliminary measurements which indicate that the plume undergoes rapid expansion to low density (order of magnitude within one exit plane diameter downstream of the exit), and (ii) an indication of what experimental parameters must be improved on, for more accurate measurements to be performed in the future. Future experimental arrangements should be improved on by use of reflective optics, specially-coated for the vacuum ultraviolet, so that the reflected-emission signal is made as intense as possible, to reduce noise in the signal.

## Acknowledgement

The measurements for this research were taken at the Air Force Research Laboratories (Edwards AFB). Support for Mark Cappelli was provided by the Air Force and the National Academy of Sciences through a summer faculty fellowship. The authors would like to thank Dr. N.B. Meezan, for his assistance in the analysis of the experimental data.

## References

1. Griem, H.R., in *Plasma Spectroscopy*, (McGraw Hill, New York), 1964, p. 174.
2. Anderson, H.M., Beregeson, S.D., Doughty, D.A., and Lawler, J.E., *Phys. Rev. A* **51**, 211, 1995.